Supporting Information

Metal-Organic Framework Based on Isonicotinate N-Oxide for Fast and Highly Efficient Aqueous Phase Cr(VI) Adsorption

Leila Aboutorabi[a], Ali Morsali[a*], Elham Tahmasebi[a] and Orhan Büyükgüngor[b]

[a]Department of Chemistry, Faculty of Basic Sciences, Tarbiat Modares University, P.O. Box 14115-175, Tehran, Iran

[b]Department of Physics, Faculty of Arts and Sciences, Ondokuz Mayis University, 55139 Kurupelit, Samsun, Turkey

Email: Morsali_a@modares.ac.ir, Morsali_a@yahoo.com

Figure S1. Optical microscopic image of TMU-30 single crystals (left) and 10 ml vial conventional heating method for synthesis the single crystals (right).

Table S1. Crystal data and structural refinement for TMU-30.

Compound number	TMU-30
Empirical formula	$C_{26}\ H_{20}\ N_5\ O_{13}\ Pb_2$
Formula weight	1024.85
Crystal system	Monoclinic
Space group	C2/c
a (Å)	27.722(3)
b (Å)	7.3936(6)
c (Å)	21.633(2)
α (°)	90.00
ß (°)	103.939 (8)
γ (°)	90.00
V (Å^3)	2993.0(5)
Z	4
D_c (g cm^{-3})	2.274
μ (mm^{-1})	11.311
Θ range (°)	1.887–26.491
Measured refls.	8233
Independent refls.	3084
R_{int}	0.1046
S	1.035
R_1/wR_2	0.0528/0.1206
$\Delta\rho_{max}/\Delta\rho_{min}$ (e Å^{-3})	2.764/-3.628
CCDC number	1440751

Table S2. Selected bond lengths (Å) and angles (˚) for TMU-30.

Pb1–O4	2.4518	Pb1–O4–O1	79.290	Pb1–O6–O2	136.039
Pb1–O1	2.4931	Pb1–O4–O6	82.178	Pb1–O6–O6	128.193
Pb1–O6	2.6367	Pb1–O4–O3	85.628	Pb1–O6–O5	71.382
Pb1–O3	2.7314	Pb1–O4–O3	137.646	Pb1–O3–O3	134.226
Pb1–O3	2.7889	Pb1–O4–O2	125.587	Pb1–O3–O2	96.329
Pb1–O2	2.7950	Pb1–O4–O2	95.307	Pb1–O3–O2	72.653
Pb1–O2	2.8058	Pb1–O4–O6	149.434	Pb1–O3–O6	71.963
Pb1–O6	2.8540	Pb1–O1–O6	73.921	Pb1–O3–O2	71.963
Pb1–O6	2.9810	Pb1–O1–O3	76.518	Pb1–O3–O2	86.449
		Pb1–O1–O3	118.102	Pb1–O3–O6	68.198
		Pb1–O1–O2	49.185	Pb1–O3–O5	93.246
		Pb1–O1–O2	149.026	Pb1–O2–O2	137.255
		Pb1–O1–O6	103.820	Pb1–O2–O6	71.606
		Pb1–O1–O6	118.686	Pb1–O2–O5	140.624
		Pb1–O6–O3	149.613	Pb1–O2–O6	66.145
		Pb1–O6–O3	68.330	Pb1–O2–O5	74.970
		Pb1–O6–O2	69.245	Pb1–O6–O5	137.332

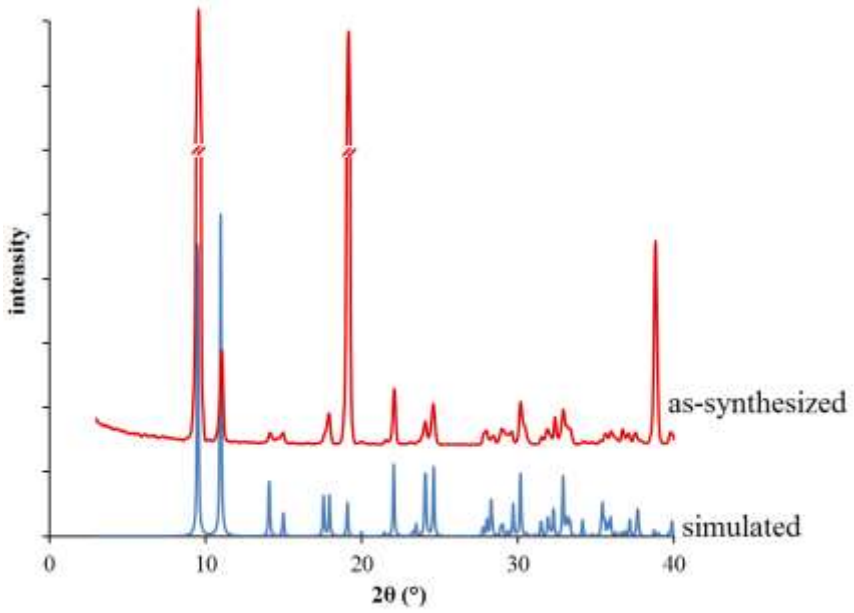

Figure S2. PXRD patterns of TMU-30.

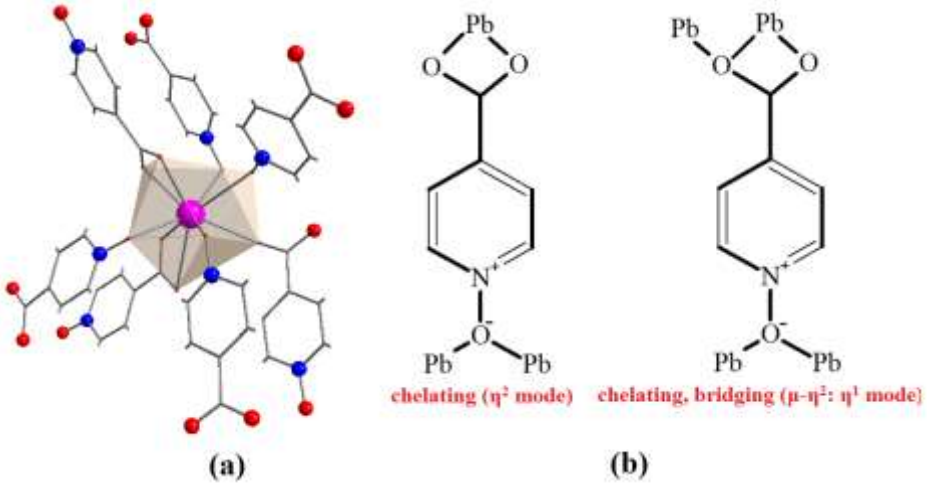

Figure S3. (a) Coordination environment around lead(II) in TMU-30; (b) the coordination mode of INO.

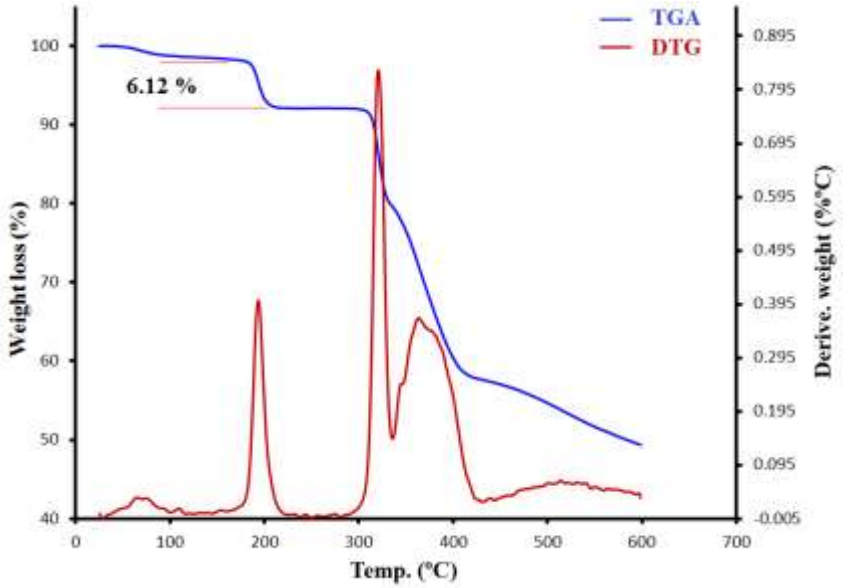

Figure S4. The TGA and DTG curves of TMU-30.

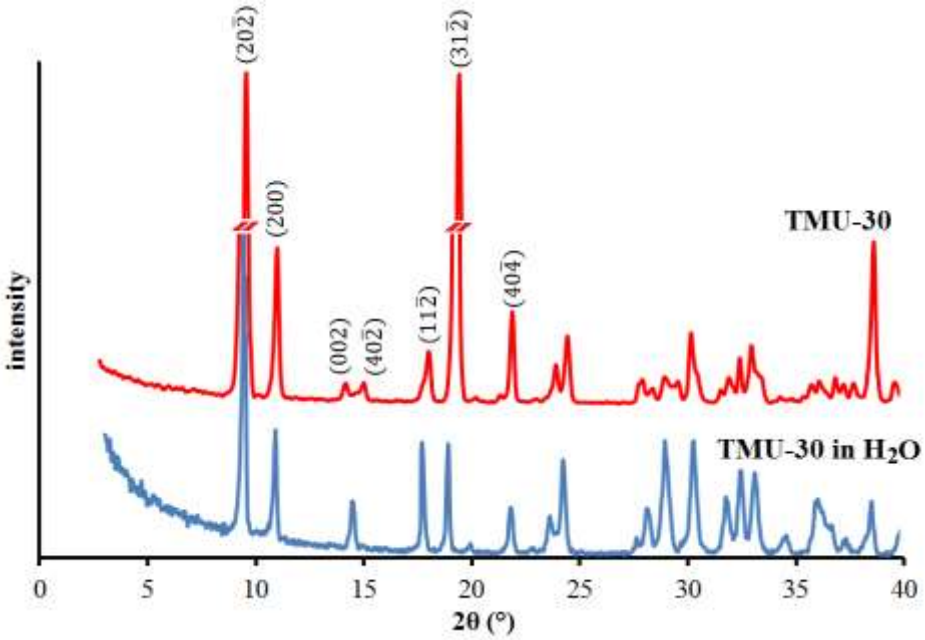

Figure S5. PXRD patterns for TMU-30 before and after immersion in H_2O for 24 h.

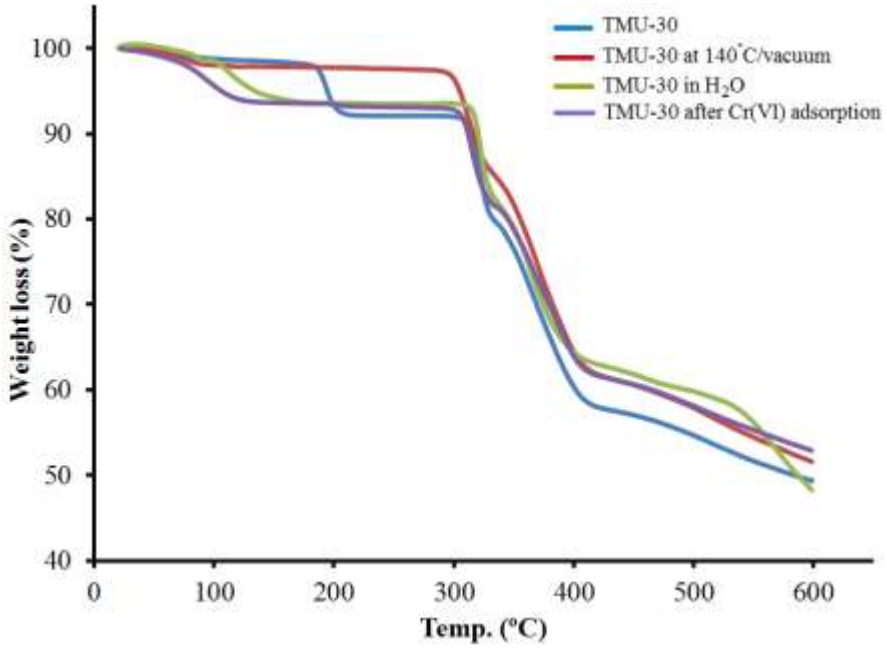

Figure S6. Comparison of TGA profiles; blue, red, green and violet solid lines showed as-synthesized TMU-30, TMU-30 at 140˚ C/vacuum, TMU-30 soaked in water for 24h and TMU-30 after Cr(VI) adsorption, respectively.

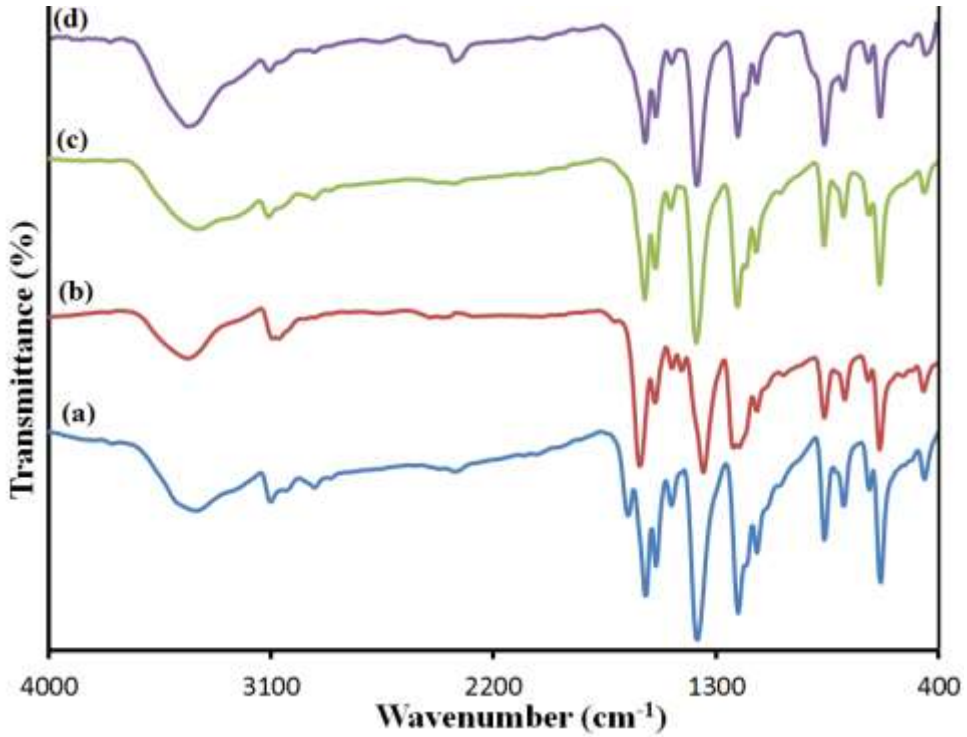

Figure S7. Comparison of FT-IR spectra; (a) as-synthesized TMU-30, (b) TMU-30 at 140˚ C/vacuum, (c) TMU-30 soaked in water for 24h and (d) TMU-30 after Cr(VI) adsorption.

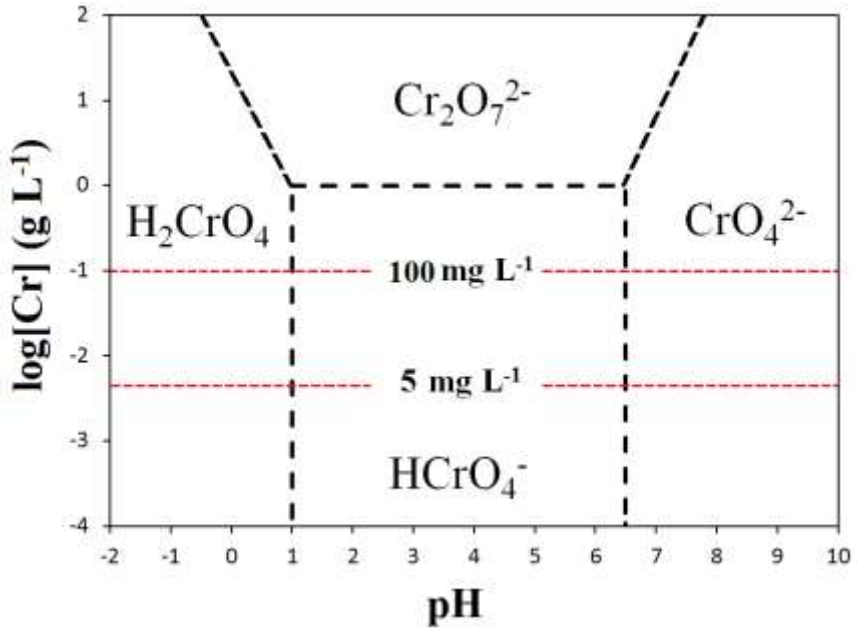

Figure S8. Predominance diagram showing the relative distribution of different Cr(VI) species in water as a function of pH and total Cr(VI) concentration.

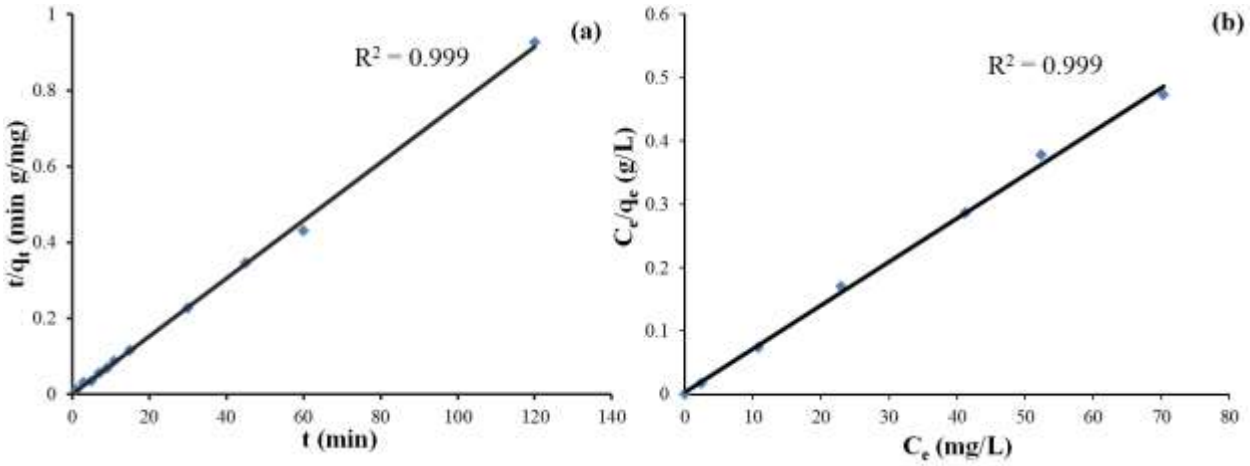

Figure S9. (a) Linear pseudo-second-order kinetic model for adsorption of Cr(VI) on the TMU-30; (Initial Cr(VI) concentration: 30 mg/L, amount of adsorbent: 10 mg, sample volume: 50 mL, pH: 5.6 and T: 298 K). (b) Langmuir linear plot; amount of adsorbent: 10 mg, contact time: 2 hours, sample volume: 50 mL, pH: 5.6 and T: 298 K.

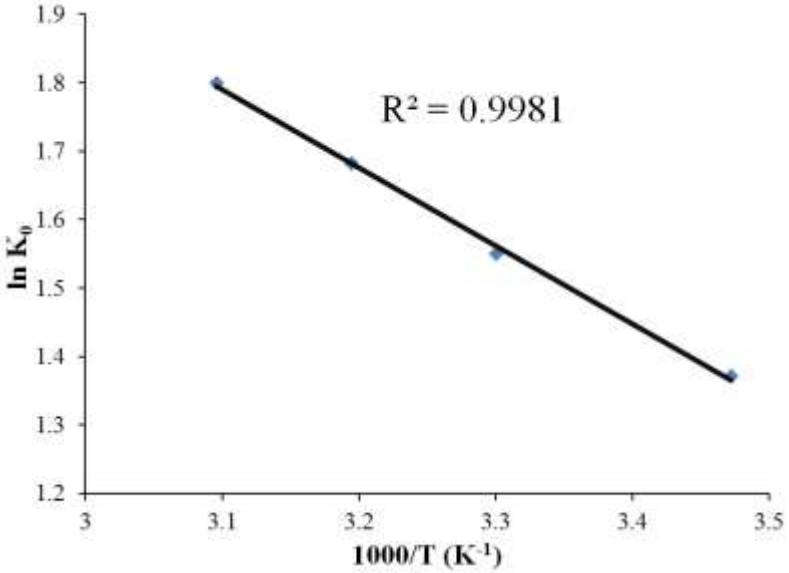

Figure S10. The plot of $\ln K_0$ *vs* 1/T.

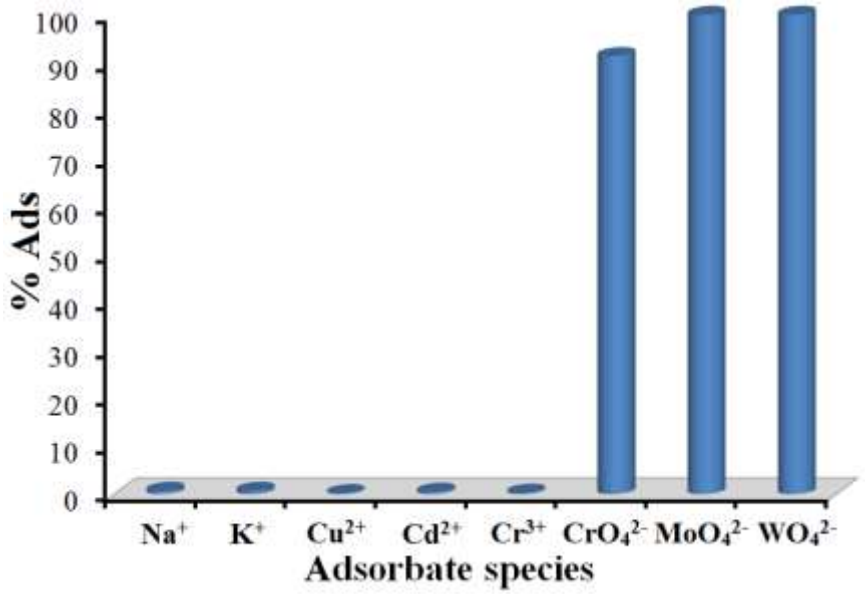

Figure S11. Adsorption of various cationic and anionic adsorbates by TMU-30.

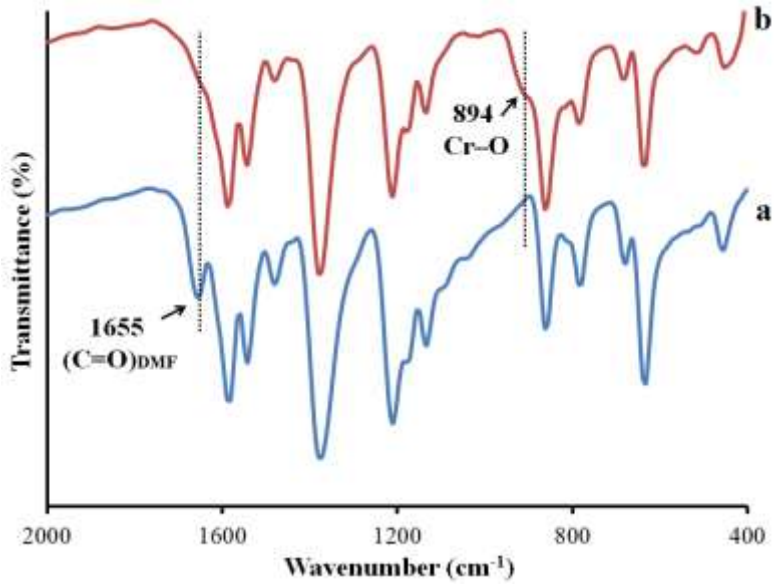

Figure S12. FT-IR spectra: (a) as-synthesized TMU-30; (b) Cr(VI)-adsorbed TMU-30.

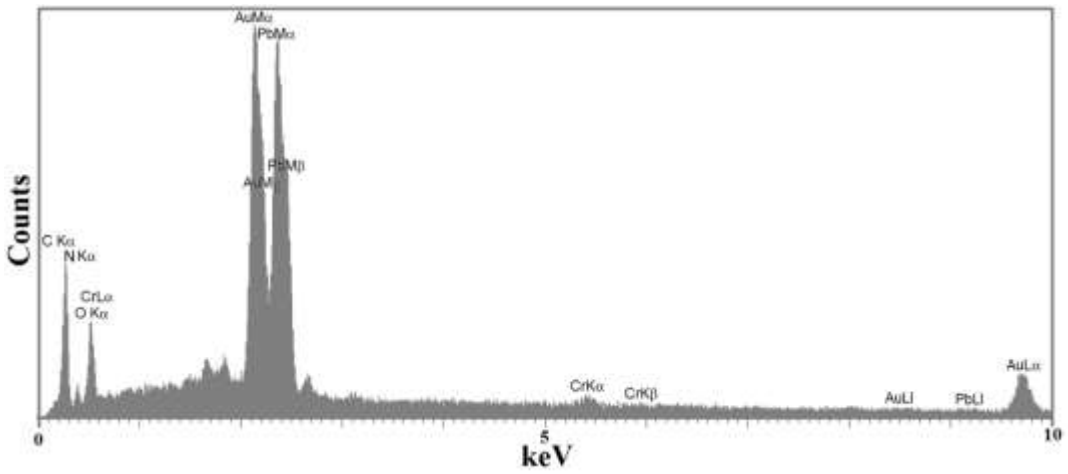

Figure S13. EDS image of Cr(VI)-adsorbed TMU-30.

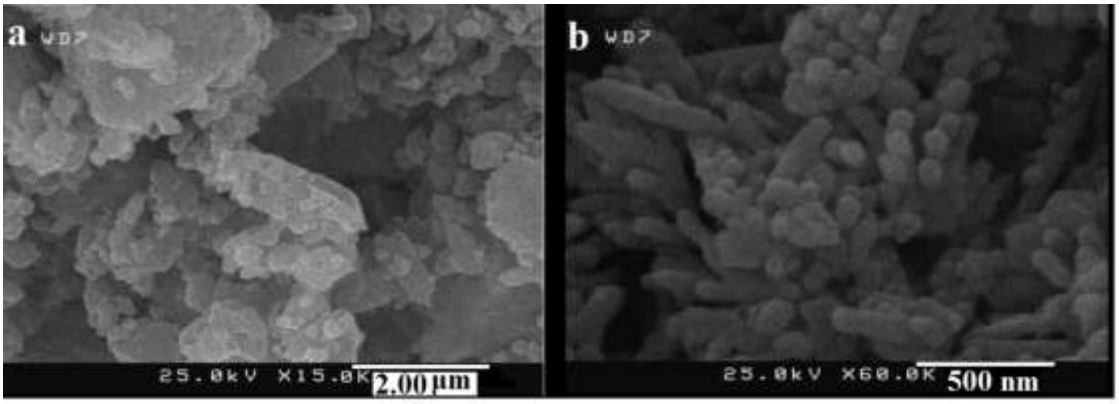

Figure S14. SEM images: (a) as-synthesized TMU-30; (b) Cr(VI)-adsorbed TMU-30.